Biotechnology Reports 31 (2021) e00645

Contents lists available at ScienceDirect

Biotechnology Reports

journal homepage: www.elsevier.com/locate/btre

Site directed confinement of laccases in a porous scaffold towards robustness and selectivity

Fangfang Yang [a], Rénal Backov [b], Jean-Luc Blin [c], Bernadett Fáklya [a], Thierry Tron [a], Yasmina Mekmouche [a,*]

[a] Aix Marseille Univ, Centrale Marseille, CNRS, iSm2, Marseille, France
[b] Université de Bordeaux, CNRS, CRPP, UMR5031, 115 Avenue Albert Schweitzer, F-33600, Pessac, France
[c] Université de Lorraine, CNRS, L2CM, F-54000 Nancy, France

ARTICLE INFO

Keywords:
Site-directed immobilization
Laccase
Heterogeneous catalysis
Orientation

ABSTRACT

We immobilized a fungal laccase with only two spatially close lysines available for functionalization into macrocellular Si(HIPE) monoliths for the purpose of continuous flow catalysis. Immobilization (30–45 % protein immobilization yields) was obtained using a covalent bond forming reaction between the enzyme and low glutaraldehyde (0.625 % (w/w)) functionalized foams. Testing primarily HBT-mediated RB5 dye decolorization in continuous flow reactors, we show that the activity of the heterogeneous catalyst is comparable to its homogeneous counterpart. More, its operational activity remains as high as 60 % after twelve consecutive decolorization cycles as well as after one-year storage, performances remarkable for such a material. We further immobilized two variants of the laccase containing a unique lysine: one located in the vicinity of the substrate oxidation site (K157) and one at the opposite side of this oxidation site (K71) to study the effect of the proximity of the Si(HIPE) surface on enzyme activity. Comparing activities on different substrates for monoliths with differentially oriented catalysts, we show a twofold discrimination for ABTS relative to ascorbate. This study provides ground for the development of neo-functionalized materials that beyond allowing stability and reusability will become synergic partners in the catalytic process.

1. Introduction

The development of new processes for a sustainable chemistry is at the heart of the great challenges of tomorrow [1]. Regarding heterogeneous catalysis, major breakthroughs are expected in terms of functionalization and surface modification as well as in the development of nano-catalysts [2]. Therefore, understanding fundamental synthesis and processing concepts in order to tailor materials while fully controlling all involved mechanistic aspects is a major task. Immobilization of enzymes on solid supports for various applications (biosensors, medical fields, biocatalyst carriers, biofuel cells, etc.) has gain a spectacular growing interest [3–7]. As for synthetic catalysts, many advantages arise from a proper enzyme immobilization such as improved operational activity, stability, reusability, selectivity, specificity (critical in resolutions of racemic mixtures), purification of enzymes or resistance to deleterious compounds [8–14]. In the absence of a specific design immobilization of proteins often leads to uncontrolled enzymes orientations which can alter the resulting activity probably due to distortion of the enzyme conformation, or a limited access to the active site and difficulty of mass transfer [15–17]. Orientation depends greatly on the nature of biocatalyst, the properties of the solid support and the method used for immobilization [18]. To minimize the above negative effects, it is meaningful to study possible orientations of a specific enzyme and select or test for a desirable one [19]. In several instances, orienting the enzyme active site was reported to improve substrate access, reduce surface effects on the active site, minimize the impact of any covalent immobilization on enzyme activity by limiting active site deformation or rigidification [20]. Addressing enzyme orientation, understanding

Abbreviations: TNC, TriNuclear Cluster; TEOS, Tetraethyl-orthosilane; APTES, (3-Aminopropyl)triethoxysilane; TTAB, tetradecyltrimethylammonium bromide; ABTS, 2,2′-azino-bis(3-ethylbenzothiazoline-6-sulfonic acid; HBT, N-Hydroxy benzotriazole; RB5, Reactive black 5; RBBR, Remazol Brilliant Blue B; Asc, ascorbic acid; S.A., specific activity; DPBS, Dulbecco's Phosphate-Buffered Saline, pH 7.0; HIPE, High Internal Phase Emulsion; Enz., enzyme; BET, Brunauer, Emmett et Teller.

* Corresponding author.
E-mail address: y.mekmouche@univ-amu.fr (Y. Mekmouche).

https://doi.org/10.1016/j.btre.2021.e00645
Received 1 April 2021; Received in revised form 4 June 2021; Accepted 7 June 2021
Available online 9 June 2021

enzyme-surface interaction and test it experimentally still remain challenging tasks especially in confined environment [21–24]. A control of enzyme orientation is increasingly important for several purposes such as methods development [25,26], biosensors and biochips [7], catalysis [15,27], electrocatalysis [21,28–32]. Amongst these developments examples of oriented enzyme immobilization in a confined environment are available thus stating the great interest of this control [12,15,16,19,33].

The enzyme laccase (EC1.10.3.2, from plant, fungi, or bacterial) is a particularly robust biocatalyst oxidizing organic substrates (tipically a phenol or an aromatic amine) at the expense of dioxygen reduction [34]. Redox reactions occur at two copper-containing centers: a surface located T1 Cu II binding center (blue copper site) responsible for the oxidation of substrate and a burried trinuclear copper T2/T3 center (TNC) responsible for the reduction of O_2 into water. In the past decades, a significant number of reports have focused on the application of this enzyme in technological and bioremediation processes [35] in addition to their use in organic synthesis [36,37] and as cathodic catalyst [38–42] reducing dioxygen into water in biofuel cells. Laccase has been successfully immobilized on many different types of support attesting for its high stability and robustness [3].

LAC3 from *Trametes* sp. C30 is a typical fungal laccase obtained in high yield as a recombinant enzyme. Mono-functionalizable variants of this laccase have been constructed by site-directed mutagenesis [43,44]. Briefly, the only two lysine groups (K_{40} and K_{71}, Fig. 1) present in the original LAC3 polypeptide chain (located opposite of the active T1 center) are first replaced by the most frequent amino acids found at these positions in other laccases (i. e. M_{40}, H_{71}) by site directed mutagenesis; the resulting lysine/free variant is then a platform for the substitution of any surface amino acid by a lysine group [44]. Next, UNIK variants (i.e. UNIque K (lysine)) graftable at a single lysine position, either in the vicinity of the T1 CuII site ($UNIK_{161}$ and $UNIK_{157}$), or in the vicinity of the T2/T3 trinuclear cluster ($UNIK_{40}$ and $UNIK_{71}$) can be constructed to assess post-functionalization of a localized engineering of the enzyme surface. Successful surface functionalizations of UNIK variants with molecules like pyrene [39], ruthenium complexes [44] or 4-ethynylbenzaldehyde [40] have been obtained in mild conditions using a reductive alkylation reaction adapted from Mc Farland and Francis [45]. It is to note that, in any case studied so far, a) the amino terminal group of the enzyme remains not affected by the grafting reaction because it is probably not accessible, b) all the modified enzymes retain a specific activity comparable to that of the parent non-modified enzyme and are stable over months (*i.e.* wet in buffered solution at 4 °C). Despite its low reactivity, surface lysine is likely to be the only exposed primary amino group prone to soft reductive amination modification [12,44].

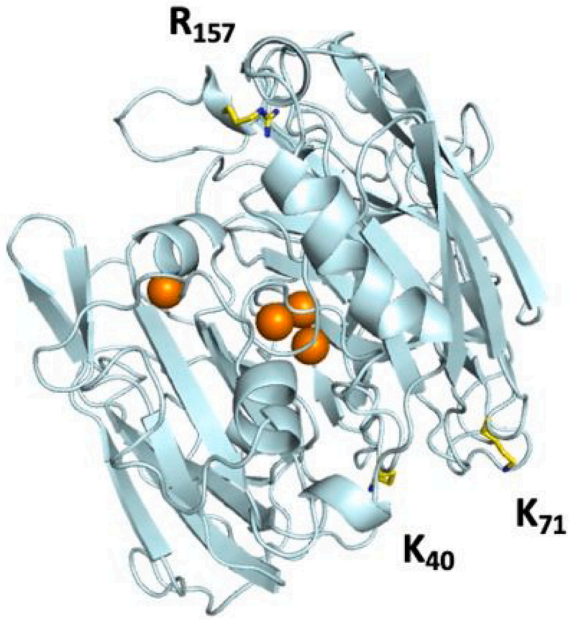

Fig. 1. Model of the structure of LAC3 with the three possible locations of lysine in either the native enzyme (K_{71} and K_{40}) or its variants $UNIK_{157}$ (R_{157} being replaced by K_{157}) and $UNIK_{71}$. View generated with PyMol. Orange balls are representing the copper ions of the active site.

Over the past decade, a variety of immobilized catalysts have been investigated including well-defined magnetic nanocatalysts, single-atom catalysts, core–shell and yolk–shell nanocatalysts, silica-based hybrid catalysts, and graphene-based materials [46–48]. Among the numerous materials available, macroporous silica offer many advantages such as straightforward synthesis, low cost, chemical stability, adjustable pore structure, and the possibility to graft a wide range of functional groups [49–51]. Its highly porous structure provides a high surface area enabling high loadings with good mass transfer rate. They are suitable materials for batch and continuous flow catalysis [49,52–56].

Glutaraldehyde is a well-known cross-linking agent for protein immobilization [10,57]. It displays a complex chemistry involving the reactive free amino groups of proteins (lysines or terminal amino group). The reaction mechanism by which glutaraldehyde reacts with proteins is not limited to one mechanism because glutaraldehyde can be found in different reactive forms (monomeric or polymeric) thus reacting differently with proteins. Indeed, it may react with proteins by several means such as aldol condensation, Schiff-base reaction, Michael-type addition, or nucleophilic attack on a cyclic hemiacetal form of the glutaraldehyde depending on pH conditions.

With glutaraldehyde preactivated support for protein post-immobilisation, Monsan and others have shown a control over the number glutaraldehyde units per amino group though a variation of glutaraldehyde concentration [58–61]. Apparently, highly activated supports (at high glutaraldehyde content, *i.e.* 10 % (w/w)) can be considered as a heterofunctional support thus promoting three different kinds of interactions with a protein: hydrophobic, anionic exchange and covalent [11]. In most cases, an ionic exchange with the amino groups in the support was shown to be the first step in the immobilization [10]. Low glutaraldehyde content (*i.e.* less than 1 % (w/w)) should lead to a weakly activated support where any primary amino group can react with only one molecule of glutaraldehyde. Accordingly, enzyme immobilization on this type of activated support should lead to the formation of a covalent bond involving the most reactive amino group on the enzyme. Although slow, immobilization will not end up reaching multipoint covalent attachment [8–10].

Here, we describe site-directed immobilization of laccases into a confined environment. We first immobilized the fungal laccase LAC3 holding with only two spacially closed surface lysines availlable for functionalization into silica macrocellular foams. Immobilization was achieved using a covalent bond formation reaction between the enzyme and a low glutaraldehyde activated silica foams (0.625 %(w/w). After evaluation of its immobilization yields, its operational activity toward periodically use or storage was primarily tested with HBT-mediated RB5 dye decolorization in continuous flow reactors. We further immobilized two laccase variants allowing for two opposite orientations through a single genetically imprinted surface functionalization site to study the effect of the proximity of the surface of a material on the enzyme activity toward different substrates. These constructions lead to a substrate oxidation site environment that is either “exposed” to the solvent or “hidden” at the enzyme/material. We show that such strategy is highly efficient for the immobilization of laccase in different orientations on silica foams while promoting stability and a high reusability of the catalysts. Influence of grafting conditions and of the enzyme orientation is discussed on the basis of the oxidation capabilities for different substrates and pH stability.

2. Materials and methods

Tetraethyl-orthosilane (TEOS), tetradecyltrimethylammonium bromide (TTAB), dodecane and hydrochloric acid (37 %), glutaradehyde Grade I 25 % in H_2O (wt. %) and (3-Aminopropyl)triethoxysilane (APTES) were purchased from Sigma. 2,2′-azino-bis(3-ethylbenzothiazoline-6-sulfonic acid (ABTS), N-Hydroxy benzotriazole (HBT), Reactive Black 5 (RB5), Remazol Brilliant Blue B (RBBR) were purchased from Fisher. All buffer solutions were made with deionized water. All other chemicals and reagents used in this study are of analytical grade and are used without any further purification.

2.1. Laccase expression and purification

Laccases from *Trametes* sp. C30 were heterologously expressed in *Aspergillus niger* and purified according to previously published procedures [43,44].

2.2. Standard enzyme assay

Protein concentration was determined by the Bradford method using BSA as standard [62], or by UV–vis spectroscopy ($\varepsilon_{610nm} = 5.6 \times 10^3$ M^{-1} cm^{-1} for the T1 copper) [63]. Laccase activity was assayed at room temperature using ABTS as substrate. Oxidation of ABTS was detected by following the absorbance at 420 nm ($\varepsilon_{420nm} = 3.6 \times 10^4$ M^{-1} cm^{-1}) during 5 min. The reaction mixture (1 mL) contained 10 µL of appropriately diluted enzyme sample and 990 µL of 5 mM ABTS freshly prepared in acetate buffer (100 mM, pH 5.7). The enzyme was added to initiate the reaction. One unit (U) of laccase was defined as one micromole of substrate oxidized per minute in these described conditions. The specific activity (S.A.) was defined as the number of unit (U) divided by the amount of laccase (mg). The molecular weight of laccase is 84 KDa [43].

2.3. Preparation of Si(HIPE), surface functionalization and characterization

HIPE stands for High Internal Phase Emulsion. HIPE silica foam was synthesized from Tetraethyl-orthosilane (TEOS), tetradecyltrimethylammonium bromide (TTAB), dodecane and hydrochloric acid (37 %) with a protocol adapted from Carn et al. [64] (Fig.**S1**−**2,** Table **S1**).

Typically, tetraethyl-orthosilane (TEOS, 5 g) were added to a 16 g of an aqueous solution of tetradecyltrimethyl ammonium bromide (TTAB) (35 % (w/w)). 5 g of 37 % HCl were then added. The aqueous solution was kept under manual stirring in a mortar for 5−10 min. After adding 35 g dodecane drop-by-drop to the above solution, the resulting emulsion was transferred into small hemolysis tubes and left for condensation at room temperature for 10 days. The resulting monoliths were washed three time with THF/acetone (1:1) and dried at room temperature. Finally, the monoliths were calcinated in an oven equipped with control temperature (650 °C for 6 h in air: 2 °C min^{-1} with a plateau at 180 °C for 2 h; the cooling temperature was driven by the oven inertia).

The silanization was achieved with a trifunctional organosilane agent, (3-aminopropyl)-triethoxysilane. APTES concentration was fixed at 2.5×10^{-3} mol g^{-1} silica foam. The silica monoliths obtained from the previous steps (approximately 75 mg each) were immerged in a 25 mL toluene/APTES solution. Dynamic vacuum was applied to force the solution into the pores of the monoliths, until effervescence stopped. Static vacuum was then maintained for overnight. After impregnation, the monoliths were taken out and washed with distilled water for three times. The obtained monoliths were dried at 80 °C for 24 h in an oven. The aminated silica foams were then immerged in a DPBS solution (pH 7.6) with glutaraldehyde (0.625 % (w/w)). As stated earlier, a dynamic vacuum firstly and an overnight static vacuum was applied for impregnation. After washing with distilled water, the silica foams were dried at 80 °C for 24 h. Materials were labelled as HCO@Si(HIPE).

Silica foam morphologies were observed by scanning electron microscopy (ZEISS Gemini SEM 500) at 3.0 kV. ^{29}Si NMR spectra were obtained by solid-state NMR spectroscopy on a Bruker Advance III WB 400 spectrometer (9.4 T). Nitrogen sorption experiments were recorded on a Micromeritics TriStar II 3020. Fourier Transform Infrared Spectroscopy measurements were assessed with a Nicolet 6700 FT-IR spectrometer.

2.4. Enzyme immobilization

The glutaraldehyde functionalized silica foam (≈ 50 mg) was immersed in 3 mL of DPBS (Dulbecco's Phosphate-Buffered Saline, pH 7.0) containing the enzyme at a desired concentration (from 50 mg L^{-1} to 2000 mg L^{-1}). The mixture was placed under vacuum in a desiccator overnight. Finally, foams were washed three times with DPBS buffer solution to remove the excess of enzyme. Immobilized LAC3, $UNIK_{157}$ and $UNIK_{71}$ are labelled as LAC3@HCO@Si(HIPE), $UNIK_{157}$@HCO@Si (HIPE) and $UNIK_{71}$@HCO@Si(HIPE) respectively.

2.5. Confirmation of enzyme-support covalent bonds

Immobilization of LAC3 and its UNIK variants was challenged by an extensive washing of grafted monoliths (1 h at 3 mL min^{-1} in a custom made circulation reactor, Fig. S3) with high ionic strength buffer (1 M NaCl) and detergent (1% Triton X100) preceded or not by a treatment with a reducing agent ($NaBH_4$). Protein content of the wash (Bradford) and the difference in enzymatic activity of the monoliths measured before and after washings were taken into consideration to evaluate enzyme leaching. Experimental details are available in the supplementary materials (§ IV. Table S2, Table S3, Table S4, Fig. S5, Fig. S6).

2.6. Dye decolorization

RB5 and RBBR dyes decolorization was followed with HBT as redox mediator. HBT was co-immobilized with laccase prior to decolorization (Supplementary Information). Functionalized monoliths were surrounded with PTFE tape and carefully introduced inside an empty plastic syringe for the substrate to flow through the foam. A recycling enzyme reactor was set up, consisting of the homemade column, a peristaltic pump, and a dye solution (25 and 50 mg L^{-1} for RB5 and RBBR respectively) dissolved in 100 mM acetate aerated buffer, pH 5.7) (Fig.**S3**). In a typical experiment, the total volume of the reaction mixture was 15 mL with a flow rate set at 3 mL min^{-1} at room temperature. Before catalysis, buffer was applied for 30 min in the whole system to wash out unbound enzyme. After each cycle, the column is disconnected and the system washed with ethanol then distilled water. Buffer is then used to wash the whole system (with the column connected). For the homogeneous conditions, 1.5 mM HBT was added in the reaction mixture with a laccase concentration was set at the same concentration of the immobilized one for comparison. Dye decolorization was evaluated by measuring the decrease of absorbance at 595 nm for RB5 and 550 nm for RBBR. Specific activity (S.A.) is defined as the number of micromoles of decolorized RB5 per min per mg of immobilized enzyme in the tested conditions. The decolorization percentage was calculated as followed:

Decolorization (%) $=[A_i\text{-}A_t/A_i]*100$, where A_i and A_t represent the initial reaction mixture absorbance and its evolution with time respectively.

2.7. Effect of the pH on enzyme activity

pH tolerance was assessed by measuring ABTS oxidation with the setup previously described. Oxidation was performed using 100 mM

acetate buffer (pH 4.0 to pH 5.7) and 100 mM sodium phosphate buffer (pH 6.0 to pH 7.0). Oxidation of ABTS was followed at 420 nm as a function of time (5 min). Molar extinction coefficient of $ABTS^{\bullet+}$ at 420 nm ($\varepsilon_{420nm} = 3.6 \times 10^4\ M^{-1}\ cm^{-1}$) was found unmodified in the pH range we tested (pH 4.0–7.0). Specific activity (S.A.) defined as the number of micromoles of ABTS radical produced per min per mg of immobilized enzyme in the tested conditions.

2.8. Dioxygen consumption

Dioxygen consumption was measured by NeoFox system using an Ocean Optics oxygen sensor probe fitted to a temperature-controlled 50 mL tube. The cycle system was set up with the ascorbic solution (100 mM) or ABTS solution (2.5 mM) in the plastic flacon. Dioxygen initial concentration was set at 250 μM at 25 °C.

3. Results and discussion

3.1. Foam preparation, LAC3 immobilization and characterization

Following a synthetic protocol previously published, we produced 3D-macrocellular Si(HIPE) monoliths bearing hierarchical porosities [64] that we successively functionalized with APTES and glutaraldehyde to obtain respectively NH_2@Si(HIPE) and HCO@Si(HIPE) monoliths (See Supplementary Information for synthetic details). Characterization of monoliths through solid state scanning electron microscopy (SEM), ^{29}Si CP-MAS NMR (Fig.**S1**, Table **S1**) as well as the evaluation of the material porosity by nitrogen physisorption (Fig.**S2**) confirmed both the nature and the structure (mesoscopic length scale) of the silica support material [65]. As expected, for HCO@Si(HIPE) materials both fully condensed Si species and incompletely condensed Si species, with a single residual hydroxyl group were observed, accounting for ≈ 9 % of the silicon atoms for 0.625 % (w/w) glutaraldehyde impregnated HCO@Si(HIPE) foams, attesting for an efficient grafting at the surface of the material. In agreement with values previously obtained for this type of foam [49,52–54], a BET surface area of ca. 600 $m^2\ g^{-1}$ accounting essentially for the microporosity was calculated for bare Si(HIPE) foams from N_2 desorption experiments (Supplementary Information). In this type of material, the surface area corresponding to the macroporosity is comparatively considered as low. It has been demonstrated that post-grafting of silane tends to block the mesoporous nodes, thus minimizing access of small molecules to the interior of the mesopores (N_2 for example). This feature can be enhanced with enzyme adjunction. As a direct consequence, it is postulated that subsequent reactions occur within the macropores [55].

To circumvent a possible leaching of adsorbed enzyme molecules, a post-functionalization of laccase was performed through Schiff-base forming reaction involving a surface exposed lysine residue (Scheme 1). The presence of only two surface located lysine residues at the surface of LAC3 (K_{40} and K_{71}) spatially close to each other (Fig. 1) ensure a similar orientation for each enzyme molecule.

The enzyme load, initially evaluated from the UV–vis spectrum of the impregnation solution (T1 copper site absorption at 610 nm ($\varepsilon_{610nm} = 5600\ M^{-1}\ cm^{-1}$), was confirmed by ICP-MS measuring the copper content in multiple samples of the grafted monoliths. Sideways, FT-IR allowed us to follow step by step the surface functionalization of the foams and the subsequent enzyme immobilization (Fig. 2A).

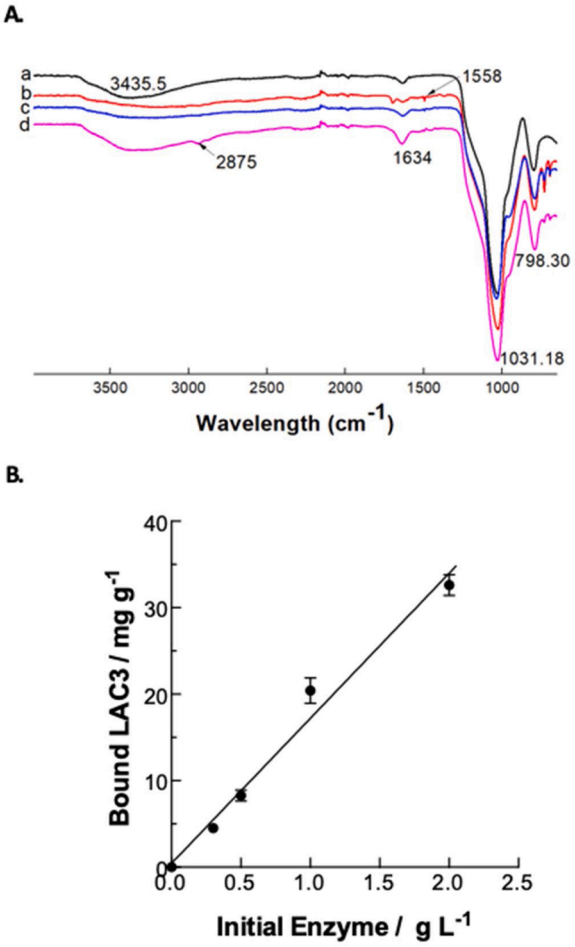

Fig. 2. Characterization of the functionalized silica foam. **A.** Infrared spectra of: (**a**) pristine silica foam; (**b**) APTES functionalized foam; (**c**) 0.625 % (w/w) glutaraldehyde functionalized foam; (**d**) LAC3 immobilized foam (8.2 mg g^{-1}). Samples were dried overnight in an oven (80 °C) prior to analysis. **B.** Laccase loads for HCO@Si(HIPE) (0.625 % (w/w) glutaraldehyde) as function of the initial enzyme concentration in the impregnation solution (see data in Table S5).

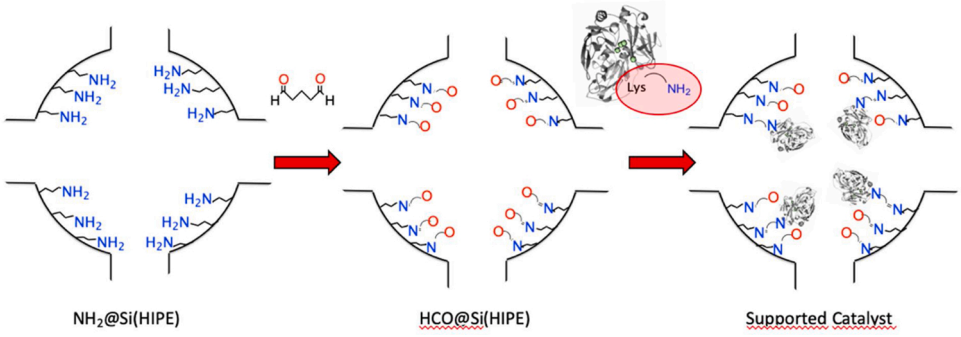

Scheme 1. Schematic representation for the immobilization strategy. The free amine groups of the NH_2@Si(HIPE) are post-functionalized with glutaraldehyde via covalent bonding forming reaction. In a second step, the enzyme is post functionalized with a second Schiff-base forming reaction. Adapted from Engström et *al.* [51].

Characteristic absorptions at 1031.18 cm^{-1} and 798.30 cm^{-1} assigned respectively to Si–O–Si asymmetric and symmetric stretching were observed for the pristine Si(HIPE) foam (Fig.2**A,a**). Bands corresponding to OH stretching mode were alsoobserved at 2400 cm^{-1} to 3600 cm^{-1} as well as that at 1634 cm^{-1}. After functionalization with APTES (NH_2@Si(HIPE)), the new peak appearing at 1558 cm^{-1} was assigned to the N—H bending vibration of the amine group (Fig. 2**A,b**). For both HCO@Si(HIPE) (Fig. 2**A,c**) and LAC3@HCO@Si(HIPE) foams (Fig. 2**A,d**), an increase in the signal at 1634 cm^{-1} assigned to C═N stretching was clearly observed demonstrating the successfulness of enzyme grafting. Moreover, after enzyme immobilization, characteristic CH_2-stretching vibration bands were visible at 2875 cm^{-1} accounting for more organic moiety attached to the silica material [52]. In order to normalize future catalytic performances to enzyme loads, enzyme immobilization was challenged at the microscopic length.

Fig. 2**B** shows the evolution of laccase loads (mass of immobilized laccase per mass unit of material) as a function of the enzyme concentration in the impregnation solution for HCO@Si(HIPE). Immobilization of LAC3 increases linearly with the concentration of the impregnating enzyme solution with no apparent saturation attesting for a good accessibility to the material. Relative to the initial laccase weight used in the impregnation solution, ca. 30 % of enzyme was retained into the HCO@Si(HIPE) after grafting and that whatever the amount of glutaraldehyde used in the pre-functionalization (Table S**5**). Glutaraldehyde-glutaraldehyde interactions can prevail on the reactivity and thus explain this limitation of grafted laccase for higher glutaraldehyde loading [66].

Challenging enzyme immobilization in monoliths through an extensive washing with a high ionic strength buffer (1 M NaCl) and a detergent (Triton X100) prior or after a treatment with a reducing agent ($NaBH_4$) resulted in less than 5% loss of the initial enzyme activity and no detectable protein in the wash solution (see Methods section and Tables S2, S3, S4). Therefore, immobilization of laccases in HCO@Si (HIPE) was considered as stable covalent bonds.

3.2. Catalytic activity of immobilized LAC3

Activity of immobilized LAC3 (8.2 mg g^{-1}) was tested on substrates with different reactivity (Fig. 3). Catalytic performance of custom made LAC3@HCO@Si(HIPE) circulation reactor (Fig.S**3**) was first evaluated following the decolorization of the industrial azo dye model RB5 in the presence of HBT as redox mediator [67] (Fig. 4, Fig.S**4**). After 24 h of circulation in the reactor, nearly 70 % of decolorization was reached, a performance comparable to that obtained in homogeneous conditions (Fig.4**A**)**.** The reactivity measured onto the support (rather than the average reactivity of differently orientated enzymes) should represent that of a preferred orientation of all immobilized LAC3 since the two surface amino acids available for grafting in LAC3 (K_{71} and K_{40}) are spatially close spatially (Fig. 1)

An important aspect distinguishing heterogeneous from homogeneous catalysis is the recyclability of the catalyst [8,68]. After ten consecutive cycles of decolorization (24 h each) the LAC3@HCO@Si (HIPE) efficiency remained within 0.75 of the homogeneous catalyst performance (Fig. 4A, Fig.S**7**)**.** This result highlights the operational stability of the heterogeneous catalyst. Similar results were repeatedly obtained with monoliths loaded with different amounts of immobilized LAC3 **(**Fig. S**7**). On the other hand, comparing a specific activity (S.A., micromoles of decolorized RB5/min/mg of LAC3) averaged from four consecutive 5 h RB5 decolorization cycles for different enzyme loads ranging from 4.9 to 34.3 mg g^{-1}, decolorization performance appeared to increase up to 8.2 mg g^{-1} immobilized LAC3 (S.A. $\approx 1.4 \times 10^{-3}$ U mg^{-1}) then rapidly decreased at higher loadings (Fig. 4B). This pattern may initially reflects an activation of laccase molecules by the carrier surface properties [69,70]. Controlling the immobilization conditions (enzyme concentration, pH, immobilization rate, ionic strength, additives, etc.) can affect the immobilized enzyme performance (activity, specificity or selectivity) [13]. Results observed for TLL, PFL and CALB lipases suggest that immobilization conditions can affect the final performance both in positive or negative way [70–72]. For example, slowing-down immobilization rate (compared to diffusion rate) of CALB reduces negative interactions between immobilized enzyme molecules by permitting a more homogeneous distribution in the pores. Therefore, covalent immobilization of LAC3 on the support can affect the observed enzyme behavior by mean of different factors like a stabilization of an active form of the enzyme or other factors related to the promotion of diffusional problems or partition of substrates or products. One possible explanation for LAC3 behavior can arise from the enzyme crowding.

Increasing LAC3 loading within our support can affect the distance between enzyme molecules so that enzyme-enzyme interaction may be affected. At low loading, distance between enzyme molecules may be too large and support effect maximal on enzyme conformation. Shortening enzyme-enzyme distances as enzyme loading increases could lead to optimal interactions for enzyme performance. Beyond an optimal loading, distances between enzymes molecules may be too short thus altering enzyme behavior and thus its efficiency. LAC3 volume was calculated to be roughly $65 \times 55 \times 45$ $Å^3$ with a diameter of ca. 67 Å, a

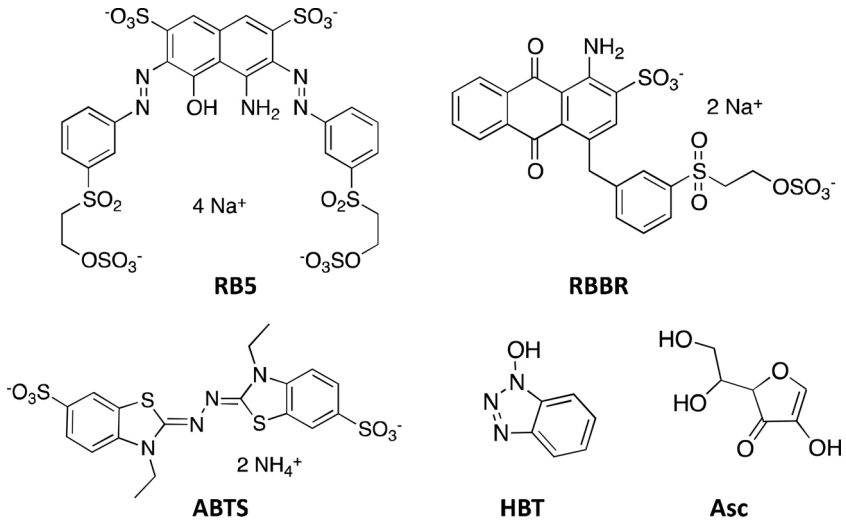

Fig. 3. Substrates and redox mediator used in this study. Reactive Black 5 (RB5) Remazol Brillant Blue R (RBBR), ABTS, Ascorbic acid (Asc) and HBT. (For interpretation of the references to colour in the Figure, the reader is referred to the web version of this article).

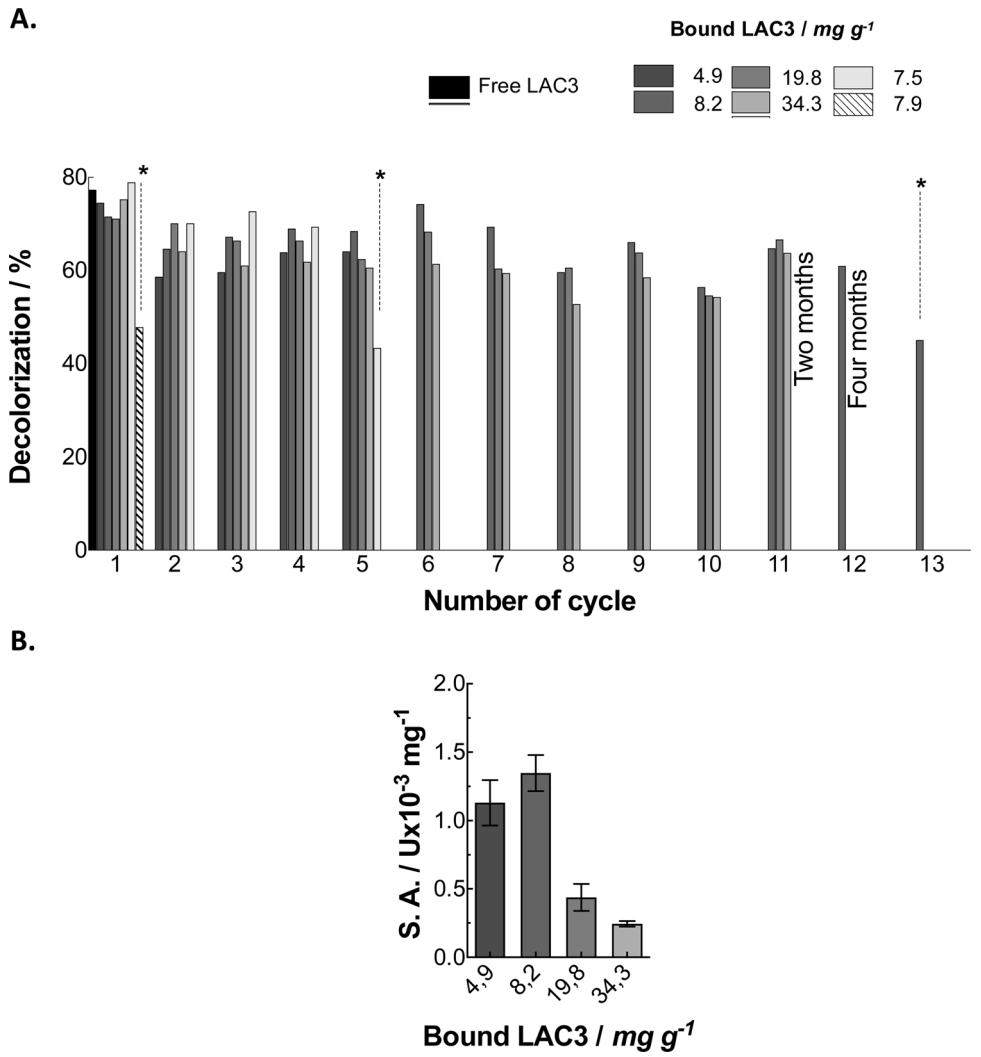

Fig. 4. Decolorization of RB5 by LAC3 immobilized onto HCO@Si(HIPE). **A.** Cycles performed with freeLAC3 and LAC3 immobilized onto HCO@Si(HIPE). * marks the performance after one year storage. **B.** Comparison of the specific activity for four averaged five hours cycles operated with 4.9, 8.2, 19.8 and 34.3 mg g^{-1} immobilized laccase (S.A. for free enzyme towards RB5 decolorization is 5.3×10^{-3} U mg^{-1}) (from Fig.S7).

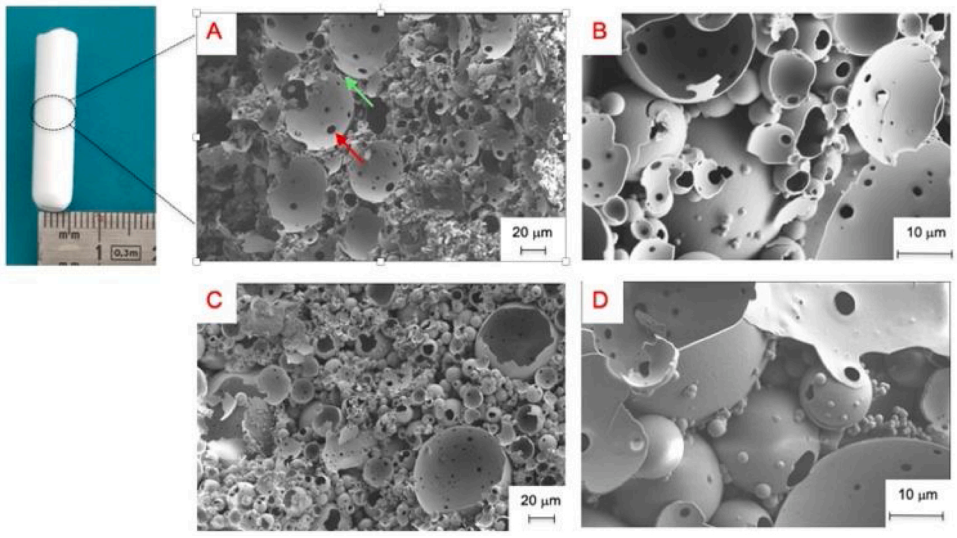

Fig. 5. SEM (Scanning Electron Microscopy) images of silica foams. **A, B**: Bare silica and C, D: LAC3-immobilized foams after four months and 10 cycles of decolorization. Red arrow: intra-wall pore opening (internal junctions); green arrow: pore-opening from the hollow sphere aggregation (external junction). Samples were dried overnight in an oven (80 °C) prior to analysis. (For interpretation of the references to colour in the Figure, the reader is referred to the web version of this article).

size perfectly suited for the porosity of the monoliths [73]. However, since the high surface area of the material is mostly describing its microporosity it is conceivable that protein-protein interactions may affect the catalysis in macropores.

Another important aspect of enzyme immobilization is the stabilization of the catalyst (Fig. 4, Fig.**S7**). Remarkably, the decolorization performance of the enzyme was found unaltered in an eleventh 24 h cycle performed after two months of periodical usage of the LAC3@HCO@Si(HIPE) monoliths (stored wet at 4 °C between 24 h cycles). For used monoliths (13 cycles), the performance was still ≈ 60 % of that of the first cycle more than a year after the first cycle (Fig. 4A). In addition, LAC3@HCO@Si(HIPE) monoliths used for only one cycle after one year storage (*i.e.* stored wet at 4 °C) still showed up≈ 60 % activity. Noteworthy, the LAC3@HCO@Si(HIPE) performances both in terms of decolorization and reusability were found similar with RBBR, a less hindered dye substrate than RB5 (Fig. 3, Fig.**S7B**). After a long-term storage and multiple decolorization cycles the integrity of the LAC3 immobilized foam was controlled by SEM. Morphological features of pristine silica monoliths were found conserved and not affected by the presence of laccase and catalysis (Fig. 5). Indeed, the typical hollow spherical aggregated structure of Si(HIPE) bearing open porosity at the surface of the macroscopic walls (internal junctions) and at the interstices between adjacent cells (external junctions) were observed in both situation [52,64]. It is important to mention that apparently no leaching of laccase had occurred as no loss of copper ion was found by ICP-MS (Table **S5**). Moreover, the $\nu_{C=N}$ stretching vibration at 1630 cm^{-1} reminiscent of an imine bond was found still present after catalysis (Fig. **S6**). The decrease in activity is apparently not a consequence of a loss in HBT as loading fresh HBT into the foam did not restore the initial activity (Fig.**S4C**). Therefore, the progressive loss of decolorization activity in our reactor appears likely attributable to a progressive inactivation of the immobilized laccase. Oxidative damage, partial denaturation of the enzyme or mechanical constraints such as brittle particle walls cracks causing an alteration of the flow are potential causes for a loss of activity.

Compared to other immobilized laccase systems, the LAC3@HCO@Si(HIPE) can be stored on a long-term basis (over one year) with almost no loss of activity and recyclability, a property for which, to the best of our knowledge, no equivalent is found in literature. In literature, operational activity of immobilized laccases may range from 60 to 90 % of that of the starting material over 20 cycles and 3 months storage [6, 36]. The closest examples are the *Alternaria tenuissima* laccase immobilized in Ca^{2+} alginate beads reported to keep 84 % activity after 42 days storage [74], the *Trametes pubescens* laccase included in chitosan beads exhibited ≈ 40 % loss after 30 days storage [75], the *Ganoderma cupreum* laccase immobilized on amino-functionalized nanosilica that showed up 84 % operational activity after 60 days storage [76] and more recently the *Trametes versicolor* laccase immobilized onto magnetic metal organic framework that showed a long-term storage of 28 days with a retention of of 88 % of its initial activity [77]. Globally, it appears that our LAC3@HCO@Si(HIPE) can maintain a substantial decolorization activity with a good reusability over a period of one year.

3.3. Comparison of LAC3 with its UNIK variants

Variations of the orientation on the material surface as well as variations in the way the enzyme is tethered can be means to modulate its activity in the foam. Grafting HCO@Si(HIPE) with the LAC3 variant $UNIK_{157}$ exposes the substrate oxidation site (materialized by the T1 copper in Fig. 1) to the material surface. To the contrary, grafting HCO@Si(HIPE) with either LAC3 or $UNIK_{71}$ exposes the substrate oxidation center to the lumen of pores. On the other hand, with only one lysine available the variant $UNIK_{71}$ offers a potentially less rigid alternative to LAC3 (K_{40}, K_{71}) for grafting HCO@Si(HIPE).

UNIK variants loads were found comparable to that of LAC3 (Table **S5**). For the two variants, the ratio of immobilized enzymes relative to the free enzyme initially present in the impregnation solution was not exceeding ≈ 40 %, a yield comparable to that obtained for LAC3. This suggests that the binding efficiency is here neither affected by the number of surface-accessible lysines nor by their location at the enzyme surface.

It is important to stress here that, for the different substrates tested in homogeneous conditions, activities of the variants are undistinguishable from those of the parental enzyme (Table **S6**) [44]. Prior comparing $UNIk_{157}$@HCO@Si(HIPE) and $UNIk_{71}$@HCO@Si(HIPE) for their RB5/HBT mediated decolorization efficiency, control experiments attesting for chemical immobilization were performed from which we conclude that, like for LAC3@HCO@Si(HIPE), >95 % of enzymes remains immobilized (Table S2,S3,S4, Fig.S5, Fig.S6). As for LAC3, their activity profile reaches a maximum between 5−10 mg of enzyme per g of foam with a decreased efficiency at higher loadings (Fig. 6). However, comparing activity at their optimum load, while the S.A. of the $UNIk_{71}$@HCO@Si(HIPE) is similar to that of the LAC3@HCO@Si(HIPE), the S.A. of the $UNIk_{157}$@HCO@Si(HIPE) appears to be ≈ 1.7 times lower. Therefore, in HBT mediated decolorization of RB5, the confinement of the substrate oxidation site at the interface with the foam surface through the functionalization of lysine 157 leads to a significant decrease of the activity of the enzyme. As supported by their similar S.A. almost twice that of $UNIk_{157}$, with both LAC3 and $UNIK_{71}$ immobilized enzymes the substrate oxidation site is similarly exposed to the pore lumen. However, the optimum is reached at a 2-times higher loading for LAC3. This effect could reflect an active site rigidification as a consequence of a multiple point anchoring of the enzyme through its two lysines 40 and 71. In order to exclude any bias linked to the Schiff-base reaction step and confirm this orientation effect, immobilization of enzymes was undertaken after an initial modification of their lysine groups. In a pre-functionalization step, we used a reductive alkylation reaction adapted from MacFarland and Francis [45] to produce the aldehyde functionalized enzymes from glutaraldehyde (Fig.**S8**). We obtained $UNIK_{71}$-CHO and $UNIK_{157}$-CHO modified enzymes with reasonable recovery yield and specific activities toward ABTS comparable to that of the non-modified enzymes (Table 1).

Specific activities for RB5 oxidation of $UNIK_{71}$-CHO and $UNIK_{157}$-CHO immobilized onto NH_2@Si(HIPE) monoliths are reported in Table 1. At similar loadings, S.A. values were found comparable for both methods (*i.e.* one step Shiff-base and two steps reductive amination followed by Schiff base) suggesting that in both cases all lysines are being involved in the grafting. For loads of 3−4 mg g^{-1} and 7−9 mg g^{-1} of immobilized enzymes, S.A. of immobilized $UNIK_{71}$-CHO represents 2–4 times that of $UNIK_{157}$-CHO. Hence, with this second functionalization method, we obtained a confirmation of the influence of the

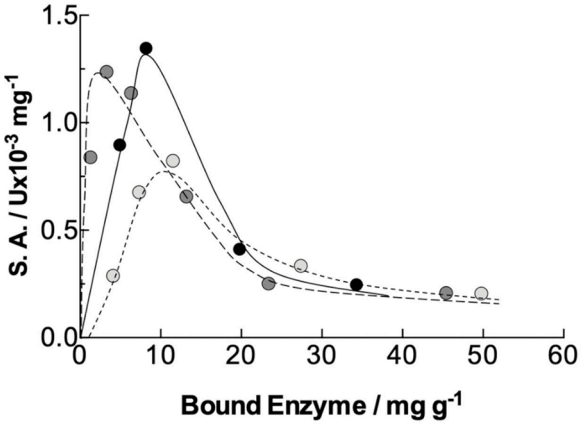

Fig. 6. Evolution of Specific activity (S.A.) as function of enzyme loads. Measures taken after three consecutive 5 h RB5 decolorization cycles. Laccases bound onto HCO@Si(HIPE): LAC3 (●), $UNIK_{71}$ (●), $UNIK_{157}$ (●). Lines are not fitting curves.

Table 1
Recovery yields, aldehyde quantification and specific activity for UNIK variants.

Enz.	Recovery yield (%)[a]	Aldehyde quantification[b]	Specific activity U mg^{-1} [c]		RB5 oxidation S.A. (x10^{-3} U mg^{-1})[d]
			Initial Enz.	Enz.-CHO	
$UNIK_{71}$	68	0.85	102	72	1.15 (1.12)[e]
$UNIK_{157}$	63	0.84	88	65	0.53 (0.33)[f]

[a] Based on CuII T1 absorption ($\varepsilon_{610nm} = 5.6 \times 10^3$ M^{-1} cm^{-1}) and compared with the initial enzyme concentration.

[b] Determined with the DNPH colorimetric assay (SI).

[c] Determined with the standard laccase assay in homogeneous conditions at pH 5.7.

[d] S.A. toward RB5 oxidation determined with Enz.-CHO post-functionalized onto NH_2@Si(HIPE) after 3 consecutive cycles: tested with 7.8 mg g^{-1} for $UNIK_{157}$-CHO immobilized and 8.6 mg g^{-1} for $UNIK_{71}$-CHO.

[e] Tested with 3.8 mg g^{-1} $UNIK_{71}$-CHO.

[f] Tested with 3.4 mg g^{-1} $UNIK_{157}$-CHO.

orientation of the enzyme at the silica matrix surface on its activity. Beyond activity, stability and reusability were not affected by the method used for grafting (one or two steps) supporting that hinderance created at the enzyme/matrix interface is the major factor influencing activity even after nine cycles and/or one year storage (Fig. **S9**). Note that, as observed for foams obtained with the previous functionalization method (one step), a $\nu_{C=N}$ stretching vibration at 1630 cm^{-1} remains present after catalysis (Fig.**S6**) suggesting the presence of a stable imine bond.

3.4. *Effect of the pH on UNIK variants activity*

Best-performing at acidic pH, laccases are known to be rapidly inhibited when hydroxyl ions accumulate (i.e. as pH increases). In order to evaluate the influence of the immobilization as well as that of the orientation of the enzyme on the pH tolerance of UNIK variants, pH dependent activities were recorded using ABTS as colorimetric substrate (ABTS is known to be stable at $4.0 < pH < 11.0$) (Fig. 7). Specific activities of both immobilized UNIK enzymes were found to be significantly lower than those of their homogeneous counterparts (see Table 1 for a comparison at pH 5.7). As expected from previous reports on laccase, the efficiency of free enzymes towards ABTS decreased rapidly as pH increased (activity at pH 6.0 < 20 % of that at pH 4.0). Immobilized, the two UNIK enzymes appear to be substantially less sensitive to pH variations than in their free forms. Thus, at pH 6.5, activity of both immobilized enzymes is ≈ 4-times that of free enzymes. Remarkably, at pH 7.0 whereas the free UNIK enzymes are not anymore active, the same enzymes immobilized still bear more than 50 % of their initial activity (Fig.7A). This modification of "pH behavior" of the enzymes after immobilization could result from local pH variations assuming the support behaves as a "solid" buffer maintaining inside the pores a pH different from that of the reaction medium [13,78]. As expected, UNIk$_{71}$@HCO@Si(HIPE) is constantly ≈ two times more active than UNIk$_{157}$@HCO@Si(HIPE) whatever the pH is(Fig.7B), suggesting that the pH dependent inhibition is not influenced by the orientation of the enzyme at the surface of the material. This is consistent with a binding of hydroxyl ions to a CuII trinuclear cluster that is deeply embedded within the protein matrix [79].

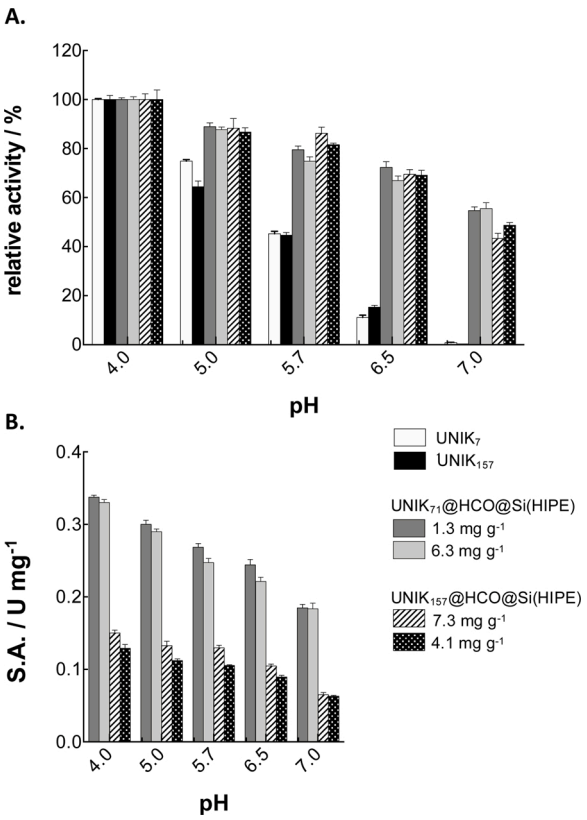

Fig. 7. pH activity profiles (ABTS oxidation) for both immobilized and free $UNIK_{71}$ and $UNIK_{157}$ laccases. **A.** Relative activity observed for each enzyme as a function of pH. 100 % is the maximum activity for each enzyme. **B.** Specific activity (S.A.) measured for immobilized $UNIK_{71}$ and $UNIK_{157}$. [ABTS] =2.5 mM. Free $UNIK_{71}$, $UNIK_{157}$, $UNIK_{71}$@HCO@Si(HIPE) (1.3 and 6.3 mg g^{-1}) and $UNIK_{157}$@HCO@Si(HIPE) (4.1 and 7.3 mg g^{-1}). Average of three independent measurements.

3.5. *O_2-dependant consumption of UNIK variants*

In order to further document on a hinderance effect at the substrate oxidation T1 copper site, assuming that no additional effect would occur at the dioxygen reduction site (TNC), dioxygen consumption measurements were performed with two substrates, i.e. ABTS and ascorbate, differing by their size (Fig.3). Ascorbate dependant O_2-consumption of $UNIK_{71}$@HCO@Si(HIPE) and $UNIK_{157}$@HCO@Si(HIPE) were found similar (9.2 ± 0.1 µM min^{-1} *vs* 8.6 ± 0.1 µM min^{-1} respectively)(Fig. **S10A**) whereas a two-fold difference was observed in kinetics as ascorbate was replaced by ABTS (Fig.**S10B**) (15.3 ± 0.2 µM min^{-1} *vs* 7.2 ± 0.2 µM min^{-1} respectively). This latter observation is consistent with the 2-fold difference in SA observed for ABTS oxidation (0.27 and 0.13 U mg^{-1} for $UNIK_{71}$@HCO@Si(HIPE) and $UNIK_{157}$@HCO@Si(HIPE) respectively). Beyond ascorbate, ABTS oxidation is likely hampered by the steric hinderance created at the interface of the enzyme and material. These results highlight the fact that the choice of the substrate is crucial in the evaluation of the activity of immobilized in two opposite enzyme orientations.

4. Conclusions

We achieved an efficient site directed immobilization of a laccase and two of its variants using Si(HIPE) foams easily functionalized through a simple Schiff base forming reaction. Activity was stable over time and reusability particularly high for a LAC3 immobilized laccase (60 % of operational activity after 12 consecutive cycles and one-year storage) attesting for a favorable and homogeneous orientation of

enzyme molecules onto the support. Using UNIK variants of LAC3 allowing to choose a single grafting point at the enzyme surface, we controled the orientation of the substrate oxidation site (next to the CuII T1) relative to the silica surface of the foam using two immobilization methods. The stability and reusability of the two immobilized variants were comparable to those of the immobilized LAC3 (e.g. at least one year storage and at least nine catalytical cycles for the immobilized $UNIK_{157}$) highlighting the gentleness of the methodology used for modifying the surface of the enzyme. From an "exposed" conformation, where the substrate oxidation site is exposed to the lumen of the monolith's pores, to a "hidden" conformation where this site is at the interface with the material within a structured hybrid open-cell system, the catalytic efficiency can be modulated. Variations observed with different substrates or pH suggest that varying the artificial environment created nearby the CuII T1 site would be an asset for tuning the reactivity of homogeneously immobilized laccase enzymes. Hence, beyond obtaining a large active surface, the support appears to be not only a matrix allowing better stability and reusability but potentially a synergic partner in the catalytic process. Extensions of this work will require to obtain insights into the structure of the enzyme confined at the material surface in order to progress in our understanding of the parameters influencing the catalytic behavior. Tailor-designed strategies will be in turn facilitated by a better understanding of confinement effects in porous materials.

Author agreements

All authors contributed to the writing, proof reading and revisions of the manuscript. All authors agree upon this submission that the manuscript has not been submitted to another journal. The authors agree on the exclusive submission with Biotechnology Reports and guarantee that there is no conflict of interests.

CRediT authorship contribution statement

Fangfang Yang, Jean-Luc Blin and Bernadett Fáklya: performed the experiment. **Rénal Backov, Thierry Tron:** Methodology, Analyzing, Reviewing, editing. **Yasmina Mekmouche:** Supervision, Methodology, Analysis, Writing.

Declaration of Competing Interest

There are no conflicts to declare.

Aknowledgements

The authors thank Elise Courvoisier-Dezord, Yolande Charmasson and the plateforme AVB for technical support. The authors thank Damien Heraud and Marius Réglier from iSm^2 for helpful discussions.

Appendix A. Supplementary data

Supplementary material related to this article can be found, in the online version, at doi:https://doi.org/10.1016/j.btre.2021.e00645.

References

[1] I.T. Horváth, Introduction: sustainable chemistry, Chem. Rev. 118 (2018) 369–371.
[2] M. Bowker, J R H Ross (ed): heterogeneous catalysis: fundamentals and applications, Catal. Lett. 142 (2012) 1411, https://doi.org/10.1007/s10562-012-0885-2.
[3] S. Datta, R. Veena, M.S. Samuel, E. Selvarajan, Immobilization of laccases and applications for the detection and remediation of pollutants: a review, Environ. Chem. Lett. 19 (2020) 521–538.
[4] C.S. Bezerra, C.M.G. de Farias Lemos, M. de Sousa, L.R.B. Gonçalves, Enzyme immobilization onto renewable polymeric matrixes: past, present, and future trends, J. Appl. Polym. Sci. 132 (2015) 42125–42140.
[5] N.A. Daronch, M. Kelbert, C.S. Pereira, P.H.H. de Araújo, D. de Oliveira, Elucidating the choice for a precise matrix for laccase immobilization: a review, Chem. Eng. J. 397 (2020) 125506–125521.
[6] M. Deska, B. Kończak, Immobilized fungal laccase as "green catalyst" for the decolourization process – state of the art, Process Biochem. 84 (2019) 112–123.
[7] Y. Liu, J. Yu, Oriented immobilization of proteins on solid supports for use in biosensors and biochips: a review, Microchim. Ichnoanal. Acta 183 (2016) 1–19.
[8] C. Mateo, J.M. Palomo, G. Fernandez-Lorente, J.M. Guisan, R. Fernandez-Lafuente, Improvement of enzyme activity, stability and selectivity via immobilization techniques, Enzyme Microb. Technol. 40 (2007) 1451–1463.
[9] O. Barbosa, R. Torres, C. Ortiz, Á. Berenguer-Murcia, R.C. Rodrigues, R. Fernandez-Lafuente, Heterofunctional supports in enzyme immobilization: from traditional immobilization protocols to opportunities in tuning enzyme properties, Biomacromolecules 14 (2013) 2433–2462.
[10] O. Barbosa, C. Ortiz, Á. Berenguer-Murcia, R. Torres, R.C. Rodrigues, R. Fernandez-Lafuente, Glutaraldehyde in bio-catalysts design: a useful crosslinker and a versatile tool in enzyme immobilization, RSC Adv. 4 (2014) 1583–1600.
[11] O. Barbosa, R. Torres, C. Ortiz, R. Fernandez-Lafuente, Versatility of glutaraldehyde to immobilize lipases: effect of the immobilization protocol on the properties of lipase b from Candida Antarctica, Process Biochem. 47 (2012) 1220–1227.
[12] K. Hernandez, R. Fernandez-Lafuente, Control of protein immobilization: coupling immobilization and site-directed mutagenesis to improve biocatalyst or biosensor performance, Enzyme Microb. Technol. 48 (2011) 107–122.
[13] R.C. Rodrigues, C. Ortiz, Á. Berenguer-Murcia, R. Torres, R. Fernández-Lafuente, Modifying enzyme activity and selectivity by immobilization, Chem. Soc. Rev. 42 (2013) 6290–6307.
[14] A. Bastida, P. Sabuquillo, P. Armisen, R. Fernandez-Lafuente, J. Huguet, J. M. Guisan, A single step purification, immobilization, and hyperactivation of lipases via interfacial adsorption on strongly hydrophobic supports, Biotechnol. Bioeng. 58 (1998) 486–493.
[15] Jd.N. Schöffer, C.R. Matte, D.S. Charqueiro, E.W. de Menezes, T.M.H. Costa, E. V. Benvenutti, R.C. Rodrigues, P.F. Hertz, Directed immobilization of cgtase: the effect of the enzyme orientation on the enzyme activity and its use in packed-bed reactor for continuous production of cyclodextrins, Process Biochem. 58 (2017) 120–127.
[16] J.R. Simons, M. Mosisch, A.E. Torda, L. Hilterhaus, Site directed immobilization of glucose-6-phosphate dehydrogenase via thiol-disulfide interchange: influence on catalytic activity of cysteines introduced at different positions, J. Biotechnol. 167 (2013) 1–7.
[17] C. Coscolín, A. Beloqui, M. Martínez-Martínez, R. Bargiela, G. Santiago, R. M. Blanco, G. Delaittre, C. Márquez-Álvarez, M. Ferrer, Controlled manipulation of enzyme specificity through immobilization-induced flexibility constraints, Appl. Catal. A Gen. 565 (2018) 59–67.
[18] J. Zdarta, A. Meyer, T. Jesionowski, M. Pinelo, A general overview of support materials for enzyme immobilization: characteristics, properties, practical utility, Catalysts 8 (2018) 92.
[19] J.C.Y. Wu, C.H. Hutchings, M.J. Lindsay, C.J. Werner, B.C. Bundy, Enhanced enzyme stability through site-directed covalent immobilization, J. Biotechnol. 193 (2015) 83–90.
[20] M. Hoarau, S. Badieyan, E.N.G. Marsh, Immobilized enzymes: understanding enzyme – surface interactions at the molecular level, Org. Biomol. Chem. 15 (2017) 9539–9551.
[21] P.V. Hitaishi, R. Clement, N. Bourassin, M. Baaden, A. De Poulpiquet, S. Sacquin-Mora, A. Ciaccafava, E. Lojou, Controlling redox enzyme orientation at planar electrodes, Catalysts 8 (2018).
[22] N. Mano, A. de Poulpiquet, O2 reduction in enzymatic biofuel cells, Chem. Rev. 118 (2018) 2392–2468.
[23] A. Küchler, M. Yoshimoto, S. Luginbühl, F. Mavelli, P. Walde, Enzymatic reactions in confined environments, Nat. Nanotechnol. 11 (2016) 409–420.
[24] J. Boudrant, J.M. Woodley, R. Fernandez-Lafuente, Parameters necessary to define an immobilized enzyme preparation, Process Biochem. 90 (2020) 66–80.
[25] Y. Li, T.L. Ogorzalek, S. Wei, X. Zhang, P. Yang, J. Jasensky, C.L. Brooks, E.N. G. Marsh, Z. Chen, Effect of immobilization site on the orientation and activity of surface-tethered enzymes, PCCP 20 (2018) 1021–1029.
[26] D. Wasserberg, J. Cabanas-Danés, J. Prangsma, S. O'Mahony, P.-A. Cazade, E. Tromp, C. Blum, D. Thompson, J. Huskens, V. Subramaniam, P. Jonkheijm, Controlling protein surface orientation by strategic placement of oligo-histidine tags, ACS Nano 11 (2017) 9068–9083.
[27] J.M. Bolivar, B. Nidetzky, Oriented and selective enzyme immobilization on functionalized silica carrier using the cationic binding module zbasic2: design of a heterogeneous d-amino acid oxidase catalyst on porous glass, Biotechnol. Bioeng. 109 (2012) 1490–1498.
[28] C. Gutiérrez-Sánchez, M. Pita, C. Vaz-Domínguez, S. Shleev, A.L. De Lacey, Gold nanoparticles as electronic bridges for laccase-based biocathodes, J. Am. Chem. Soc. 134 (2012) 17212–17220.
[29] V. Balland, C. Hureau, A.M. Cusano, Y. Liu, T. Tron, B. Limoges, Oriented immobilization of a fully active monolayer of histidine-tagged recombinant laccase on modified gold electrodes, Chemistry 14 (2008) 7186–7192.
[30] C.F. Blanford, C.E. Foster, R.S. Heath, F.A. Armstrong, Efficient electrocatalytic oxygen reduction by the 'blue' copper oxidase, laccase, directly attached to chemically modified carbons, Faraday Discuss 140 (2009) 319–335.
[31] C.F. Blanford, R.S. Heath, F.A. Armstrong, A stable electrode for high-potential, electrocatalytic o2 reduction based on rational attachment of a blue copper oxidase to a graphite surface, Chem. Commun. (2007) 1710–1712.

[32] L. dos Santos, V. Climent, C.F. Blanford, F.A. Armstrong, Mechanistic studies of the 'blue' cu enzyme, bilirubin oxidase, as a highly efficient electrocatalyst for the oxygen reduction reaction, PCCP 12 (2010) 13962–13974.
[33] G. Cottone, S. Giuffrida, S. Bettati, S. Bruno, B. Campanini, M. Marchetti, S. Abbruzzetti, C. Viappiani, A. Cupane, A. Mozzarelli, L. Ronda, More than a confinement: "Soft" and "hard" enzyme entrapment modulates biological catalyst function, Catalysts 9 (2019) 1024.
[34] Bookmatter_ Encyclopedia of Metalloproteins, Springer, New York, NY, 2013.
[35] D.M. Mate, M. Alcalde, Laccase: A multi-purpose biocatalyst at the forefront of biotechnology, Microb. Biotechnol. 10 (2017) 1457–1467.
[36] T. Kudanga, B. Nemadziva, M. Le Roes-Hill, Laccase catalysis for the synthesis of bioactive compounds, Appl. Microbiol. Biotechnol. 101 (2017) 13–33.
[37] S. Riva, Laccases: Blue enzymes for green chemistry, Trends Biotechnol. 24 (2006) 219–226.
[38] A. Franco, S. Cebrián-García, D. Rodríguez-Padrón, A.R. Puente-Santiago, M. J. Muñoz-Batista, A. Caballero, A.M. Balu, A.A. Romero, R. Luque, Encapsulated laccases as effective electrocatalysts for oxygen reduction reactions, ACS Sus. Chem. Eng. 6 (2018) 11058–11062.
[39] S. Gentil, P. Rousselot-Pailley, F. Sancho, V. Robert, Y. Mekmouche, V. Guallar, T. Tron, A. Le Goff, Efficiency of site-specific clicked laccase–carbon nanotubes biocathodes towards o2 reduction, Chem. Eur. J. 26 (2020) 4798–4804.
[40] N. Lalaoui, P. Rousselot-Pailley, V. Robert, Y. Mekmouche, R. Villalonga, M. Holzinger, S. Cosnier, T. Tron, A. Le Goff, Direct electron transfer between a site-specific pyrene-modified laccase and carbon nanotube/gold nanoparticle supramolecular assemblies for bioelectrocatalytic dioxygen reduction, ACS Catal. 6 (2016) 1894–1900.
[41] A.A. Arrocha, U. Cano-Castillo, S.A. Aguila, R. Vazquez-Duhalt, Enzyme orientation for direct electron transfer in an enzymatic fuel cell with alcohol oxidase and laccase electrodes, Biosens. Bioelectron. 61 (2014) 569–574.
[42] J. Martinez-Ortiz, R. Flores, R. Vazquez-Duhalt, Molecular design of laccase cathode for direct electron transfer in a biofuel cell, Biosens. Bioelectron. 26 (2011) 2626–2631.
[43] Y. Mekmouche, S. Zhou, A.M. Cusano, E. Record, A. Lomascolo, V. Robert, A. J. Simaan, P. Rousselot-Pailley, S. Ullah, F. Chaspoul, T. Tron, Gram-scale production of a basidiomycetous laccase in aspergillus niger, J. Biosci. Bioeng. 117 (2014) 25–27.
[44] V. Robert, E. Monza, L. Tarrago, F. Sancho, A. De Falco, L. Schneider, E. Npetgat Ngoutane, Y. Mekmouche, P.R. Pailley, A.J. Simaan, V. Guallar, T. Tron, Probing the surface of a laccase for clues towards the design of chemo-enzymatic catalysts, ChemPlusChem 82 (2017) 607–614.
[45] J.M. McFarland, M.B. Francis, Reductive alkylation of proteins using iridium catalyzed transfer hydrogenation, J. Am. Chem. Soc. 127 (2005) 13490–13491.
[46] F. Zaera, Nanostructured materials for applications in heterogeneous catalysis, Chem. Soc. Rev. 42 (2013) 2746–2762.
[47] C.J. Shearer, A. Cherevan, D. Eder, Application and future challenges of functional nanocarbon hybrids, Adv. Mater. 26 (2014) 2295–2318.
[48] E. Gross, J.H.-C. Liu, F.D. Toste, G.A. Somorjai, Control of selectivity in heterogeneous catalysis by tuning nanoparticle properties and reactor residence time, Nat. Chem. 4 (2012) 947–952.
[49] N. Brun, S. Ungureanu, H. Deleuze, R. Backov, Hybrid foams, colloids and beyond: from design to applications, Chem. Soc. Rev. 40 (2011) 771–788.
[50] A. Roucher, M. Depardieu, D. Pekin, M. Morvan, R. Backov, Inorganic, hybridized and living macrocellular foams: "Out of the box" heterogeneous catalysis, Chem. Rec. 18 (2018) 776–787.
[51] K. Engström, E.V. Johnston, O. Verho, K.P.J. Gustafson, M. Shakeri, C.-W. Tai, J.-E. Bäckvall, Co-immobilization of an enzyme and a metal into the compartments of mesoporous silica for cooperative tandem catalysis: an artificial metalloenzyme, Angew. Chem. Int. Ed. 52 (2013) 14006–14010.
[52] A. Roucher, E. Roussarie, R.M. Gauvin, J. Rouhana, S. Gounel, C. Stines-Chaumeil, N. Mano, R. Backov, Bilirubin oxidase-based silica macrocellular robust catalyst for on line dyes degradation, Enzyme Microb. Technol. 120 (2019) 77–83.
[53] N. Brun, A. Babeau-Garcia, M.-F. Achard, C. Sanchez, F. Durand, G. Laurent, M. Birot, H. Deleuze, R. Backov, Enzyme-based biohybrid foams designed for continuous flow heterogeneous catalysis and biodiesel production, Energy Environ. Sci. 4 (2011) 2840–2844.
[54] D.P. Debecker, Innovative sol-gel routes for the bottom-up preparation of heterogeneous catalysts, Chem. Rec. 18 (2018) 662–675.
[55] N. Brun, A. Babeau Garcia, H. Deleuze, M.F. Achard, C. Sanchez, F. Durand, V. Oestreicher, R. Backov, Enzyme-based hybrid macroporous foams as highly efficient biocatalysts obtained through integrative chemistry, Chem. Mater. 22 (2010) 4555–4562.
[56] L. van den Biggelaar, P. Soumillion, D.P. Debecker, Biocatalytic transamination in a monolithic flow reactor: improving enzyme grafting for enhanced performance, RSC Adv. 9 (2019) 18538–18546.
[57] I. Migneault, C. Dartiguenave, M.J. Bertrand, K.C. Waldron, Glutaraldehyde: Behavior in aqueous solution, reaction with proteins, and application to enzyme crosslinking, BioTechniques 37 (2004) 790–802.
[58] P. Monsan, Optimization of glutaraldehyde activation of a support for enzyme immobilization, J. Mol. Catal. 3 (1978) 371–384.
[59] L. Betancor, F. López-Gallego, A. Hidalgo, N. Alonso-Morales, G.D.-O.C. Mateo, R. Fernández-Lafuente, J.M. Guisán, Different mechanisms of protein immobilization on glutaraldehyde activated supports: effect of support activation and immobilization conditions, Enzyme Microb. Technol. 39 (2006) 877–882.
[60] Q. Shi, J. Chen, Y. Wang, Z. Li, X. Li, C. Sun, L. Zheng, Immobilization of cyclooxygenase-2 on silica gel microspheres: optimization and characterization, Molecules 20 (2015) 19971–19983.
[61] F. López-Gallego, L. Betancor, C. Mateo, A. Hidalgo, N. Alonso-Morales, G. Dellamora-Ortiz, J.M. Guisán, R. Fernández-Lafuente, Enzyme stabilization by glutaraldehyde crosslinking of adsorbed proteins on aminated supports, J. Biotechnol. 119 (2005) 70–75.
[62] M.M. Bradford, A rapid and sensitive method for the quantitation of microgram quantities of protein utilizing the principle of protein-dye binding, Anal. Biochem. 72 (1976) 248–254.
[63] D.J. Kosman, Redox cycling in iron uptake, efflux, and trafficking, J. Biol. Chem. 285 (2010) 26729–26735.
[64] F. Carn, A. Colin, M.-F. Achard, H. Deleuze, E. Sellier, M. Birot, R. Backov, Inorganic monoliths hierarchically textured via concentrated direct emulsion and micellar templates, J. Mater. Chem. 14 (2004) 1370–1376.
[65] L. Nicole, C. Boissière, D. Grosso, A. Quach, C. Sanchez, Mesostructured hybrid organic–inorganic thin films, J. Mater. Chem. 15 (2005) 3598–3627.
[66] I. Migneault, C. Dartiguenave, M.J. Bertrand, K.C. Waldron, Glutaraldehyde: behavior in aqueous solution, reaction with proteins, and application to enzyme crosslinking, BioTechniques 37 (790-6) (2004) 798–802.
[67] P. Reyes, M. Pickard, R. Vazquez-Duhalt, Hydroxybenzotriazole increases the range of textile dyes decolorized by immobilized laccase, Biotechnol. Lett. 21 (1999) 875–880.
[68] R.C. Rodrigues, Á. Berenguer-Murcia, R. Fernandez-Lafuente, Coupling chemical modification and immobilization to improve the catalytic performance of enzymes, Adv. Synth. Catal. 353 (2011) 2216–2238.
[69] D.-H. Zhang, L.-X. Yuwen, L.-J. Peng, Parameters affecting the performance of immobilized enzyme, J. Chem. 2013 (2013) 1–7.
[70] S. Arana-Peña, N.S. Rios, D. Carballares, C. Mendez-Sanchez, Y. Lokha, L.R. B. Gonçalves, R. Fernandez-Lafuente, Effects of enzyme loading and immobilization conditions on the catalytic features of lipase from pseudomonas fluorescens immobilized on octyl-agarose beads, Front. Bioeng. Biotechnol. 8 (2020).
[71] H. Zaak, E.-H. Siar, J.F. Kornecki, L. Fernandez-Lopez, S.G. Pedrero, J.J. Virgen-Ortíz, R. Fernandez-Lafuente, Effect of immobilization rate and enzyme crowding on enzyme stability under different conditions. The case of lipase from thermomyces lanuginosus immobilized on octyl agarose beads, Process Biochem. 56 (2017) 117–123.
[72] L. Fernandez-Lopez, S. Garcia Pedrero, N. Lopez-Carrobles, B. Gorines, J. Virgen-Ortíz, R. Fernandez-Lafuente, Effect of protein load on stability of immobilized enzymes, Enzyme Microb. Technol. 98 (2017) 18–25.
[73] K. Piontek, M. Antorini, T. Choinowski, Crystal structure of a laccase from the fungus trametes versicolor at 1.90-a resolution containing a full complement of coppers, J. Biol. Chem. 277 (2002) 37663–37669.
[74] A.A. Abd El Aty, F.A. Mostafa, M.E. Hassan, E.R. Hamed, M.A. Esawy, Covalent immobilization of alternaria tenuissima km651985 laccase and some applied aspects, Biocatal. Agric. Biotechnol. 9 (2017) 74–81.
[75] H.-F. Ma, G. Meng, B.-K. Cui, J. Si, Y.-C. Dai, Chitosan crosslinked with genipin as supporting matrix for biodegradation of synthetic dyes: laccase immobilization and characterization, Chem. Eng. Res. Des. 132 (2018) 664–676.
[76] M. Gahlout, D.M. Rudakiya, S. Gupte, A. Gupte, Laccase-conjugated amino-functionalized nanosilica for efficient degradation of reactive violet 1 dye, Int. Nano Lett. 7 (2017) 195–208.
[77] A. Amari, F.M. Alzahrani, N.S. Alsaiari, K.M. Katubi, F.B. Rebah, M.A. Tahoon, Magnetic metal organic framework immobilized laccase for wastewater decolorization, Processes 9 (2021) 774.
[78] J.M. Guisán, G. Alvaro, C.M. Rosell, R. Fernandez-Lafuente, Industrial design of enzymic processes catalysed by very active immobilized derivatives: utilization of diffusional limitations (gradients of ph) as a profitable tool in enzyme engineering, Biotechnol. Appl. Biochem. 20 (1994) 357–369.
[79] S.M. Jones, E.I. Solomon, Electron transfer and reaction mechanism of laccases, Cell. Mol. Life Sci. CMLS 72 (2015) 869–883.